ARMY RESEARCH LABORATORY

Magnesium Nanocomposites: Current Status and Prospects for Army Applications

by Vincent H. Hammond

ARL-TR-5728 September 2011

NOTICES

Disclaimers

The findings in this report are not to be construed as an official Department of the Army position unless so designated by other authorized documents.

Citation of manufacturer's or trade names does not constitute an official endorsement or approval of the use thereof.

Destroy this report when it is no longer needed. Do not return it to the originator.

Army Research Laboratory
Aberdeen Proving Ground, MD 21005-5069

ARL-TR-5728 **September 2011**

Magnesium Nanocomposites: Current Status and Prospects for Army Applications

Vincent H. Hammond
Weapons and Materials Research Directorate, ARL

REPORT DOCUMENTATION PAGE	Form Approved OMB No. 0704-0188

1. REPORT DATE *(DD-MM-YYYY)*	2. REPORT TYPE	3. DATES COVERED (From - To)
September 2011	Final	

4. TITLE AND SUBTITLE	5a. CONTRACT NUMBER
Magnesium Nanocomposites: Current Status and Prospects for Army Applications	5b. GRANT NUMBER
	5c. PROGRAM ELEMENT NUMBER

6. AUTHOR(S)	5d. PROJECT NUMBER
Vincent H. Hammond	5e. TASK NUMBER
	5f. WORK UNIT NUMBER

7. PERFORMING ORGANIZATION NAME(S) AND ADDRESS(ES)	8. PERFORMING ORGANIZATION REPORT NUMBER
U.S. Army Research Laboratory ATTN: RDRL-WMM-F 4600 Loop Deer Creek Loop Aberdeen Proving Ground MD 21005-5069	ARL-TR-5728

9. SPONSORING/MONITORING AGENCY NAME(S) AND ADDRESS(ES)	10. SPONSOR/MONITOR'S ACRONYM(S)
	11. SPONSOR/MONITOR'S REPORT NUMBER(S)

12. DISTRIBUTION/AVAILABILITY STATEMENT

Approved for public release; distribution unlimited.

13. SUPPLEMENTARY NOTES

14. ABSTRACT

Due to their low density and high specific properties, the interest in magnesium (Mg) alloys for lightweight structural applications has steadily increased over the last decade. Nevertheless, their use remains limited due to poor room temperature ductility, low elastic modulus, and poor performance at elevated temperature. Recently, however, the use of nano-sized reinforcements has resulted in appreciable improvements in the performance of Mg alloys at both ambient and elevated temperatures.

In an effort to provide a brief introduction into Mg-based nanocomposites, this report surveys the current state of research in these materials. The report begins with a review of the two major processing methods used to produce the nanocomposites. Next, the impact of nanoreinforcements on a broad array of mechanical and physical properties is discussed. Of particular interest in this section is the influence of nanoparticle type and processing method on tensile. The report concludes with some observations regarding the potential use of these materials in Army-related applications.

15. SUBJECT TERMS

Mg, nanocomposites, nanoreinforcements, tensile strength, compressive strength

16. SECURITY CLASSIFICATION OF:			17. LIMITATION OF ABSTRACT	18. NUMBER OF PAGES	19a. NAME OF RESPONSIBLE PERSON
a. REPORT	b. ABSTRACT	c. THIS PAGE	UU	38	Vincent H. Hammond
UNCLASSIFIED	UNCLASSIFIED	UNCLASSIFIED			19b. TELEPHONE NUMBER (*Include area code*) (410) 306-0855

Contents

List of Figures

List of Tables

1. Introduction

The continued drive to develop lightweight materials suitable for structural use has resulted in a renewed focus on magnesium (Mg) due to its low density and resulting high specific properties. As a result, the world production of Mg has increased by approximately 100% over the last 10 years. However, several factors have hindered the widespread use of commercially pure Mg for many engineering applications. One critical issue is an inherent brittleness due to the hexagonal close-packed crystal structure of Mg at room temperature. Such brittleness necessarily limits the amount of cold working that can be performed on Mg alloys. As a result, any working that needs to be done after casting and/or molding must be done above 225 °C (where Mg has good deformation behavior), thereby resulting in increased processing time and cost. An additional limiting factor is low toughness resulting from shrinkage-induced microporosity that typically occurs during casting and/or cooling (*1*). Finally, commercially pure Mg has poor corrosion resistance and a relatively high thermal expansion coefficient (about 10% higher than aluminum), both of which are concerns for many design engineers.

Many of the identified problems have been successfully addressed through the addition of various alloying elements. For example, aluminum has been a primary alloying element since the 1920s, as it is found to increase the tensile strength through the formation of reinforcing intermetallic phase $Mg_{17}Al_{12}$. Rare earth elements (such as yttrium (Y) or neodymium (Nd)) have increased in use, as they impart significant property improvements due to precipitation hardening. Improvements in corrosion resistance have been obtained through the development of high purity alloys that severely limit the amount of iron (Fe), nickel (Ni), or copper (Cu) present in the alloy. Continued metallurgical investigations routinely produce Mg alloys with improved properties that are suitable for a broad range of applications.

Although alloying and precipitation hardening typically improve the performance of alloys relative to the base metal, there are applications where the property improvements obtained through such methods are still not sufficient. The next step of property improvements has been achieved through the development of Mg matrix composites in which reinforcements such as particulates, whiskers, and/or fibers are used. The most common types of reinforcements have been ceramics, such as silicon carbide (SiC), yttria (Y_2O_3), or alumina (Al_2O_3), as well as the intermetallic compound Mg_2Si. In these composites, the reinforcement size is typically on the order of 2–20 microns. However, results on these composites systems indicated that tensile properties tended to decrease as the particle size increased. Ye and Liu have recently published a thorough review on the status of Mg composites (*2*).

Within the last decade, attention has focused on the use of nanoparticles reinforcements in both pure Mg and Mg alloys. Typically, the reinforcement is a hard ceramic, such as Al_2O_3, Y_2O_3, SiC, or SiO_2, although metallic nanoparticles have also been used. Nano-sized reinforcements act

to refine the grain size of the matrix and introduce stress fields due to the mismatch in coefficient of thermal expansion. Both of these effects inhibit dislocation motion, thereby increasing the strength of the nanocomposites. Furthermore, in the majority of reports surveyed for this review, the incorporation of a small amount (~1% by volume) of nano-sized reinforcements generally resulted in an increase in tensile ductility.

In view of the improved properties and potential applications for nanoreinforced Mg, this report will summarize the current state of research efforts in this area. The first section will address the processing methods that have been used to fabricate these composites. Next, the mechanical performance of these composites will be addressed, primarily grouped according to the property of interest. Finally, a brief discussion on the potential of these materials for Army-related applications will be presented.

2. Processing of Mg Nanocomposites

Not surprisingly, the majority of efforts to produce nanoreinforced Mg have employed methods already in place for producing particulate reinforced alloys. That said, however, recent efforts have explored novel processing techniques designed to achieve better nanoparticle dispersion or minimize costs associated with incorporating the nanoparticles. Broadly classified, these methods can be divided into two main categories: powder-based processing and melt-based processing. Each will be discussed in turn.

2.1 Powder-based Processing

In the powder-based methods, the initial powders are mixed together in an effort to achieve the desired composition and uniform dispersion of the reinforcements in the Mg matrix. The powders are typically then pressed into billets and sintered to (nearly) full density. An important advantage of this approach is that there is essentially no limit regarding composition or reinforcement content. As a result, such an approach allows for combinations of matrix and reinforcement that cannot be produced through melt-based processing.

In mechanical alloying, the powder and milling media are placed into mixing vessels that are agitated in a high-energy milling machine. During the mixing process, the powder particles undergo repeated cycles of cold welding and fracturing of interparticle bonds. At the end of the process, the powder has been alloyed to the desired composition. Although typically used to produce oxide-dispersion-strengthened nickel and iron superalloys, mechanical alloying has also been used to produce TiC nanoparticle (3–7 nm)-reinforced Mg (*3*).

In contrast to mechanical alloying, a technique known as the blend-press-sinter (BPS) method has been used extensively (*4–15*). In this method, Mg alloy and nanopowders are blended for an extended period of time to ensure the even dispersion of the ceramic powder. Once blended, the

powders are typically cold pressed to form a green compact, which is then sintered at moderate temperature (400–500 °C) in an argon (Ar) atmosphere. The sintered piece is then extruded at a temperature ranging from 250–400 °C to form specimens suitable for testing and characterization. Representative micrographs of pure Mg reinforced with either alumina or zirconia (ZrO_2) are shown in figure 1. A minor variation on this technique is one in which the sintering step is bypassed; that is, the green compact is simply extruded rather than sintered (*16*). The primary difference between this method and mechanical alloying is that no milling media are used for BPS, so the mixing step in BPS is not as energetic as in mechanical alloying.

Microwave sintering represents an alternative to conventional sintering used in the BPS processing method. In microwave sintering, the sample is rapidly heated to 80% (or higher) of the melting temperature using a high powered microwave oven, rather than external radiant heating. In such an approach, energy is only needed to heat the part and not the furnace, thereby offering significant cost savings, as well as shorter processing times. Researchers have used 100% microwave sintering—in addition to a hybrid approach—in which the sample was heated directly by microwaves and heat transferred from a microwave-heated susceptor to produce samples with near theoretical densities (*11, 17–20*). The combination of rapid heating rates and extremely high temperature can reduce the total sintering time up to 90% relative to the conventional sintering process. Equally important, parts sintered in this fashion achieve similar densities as conventionally sintered parts while displaying improved mechanical properties (yield strength, ultimate strength, ductility) (*17*).

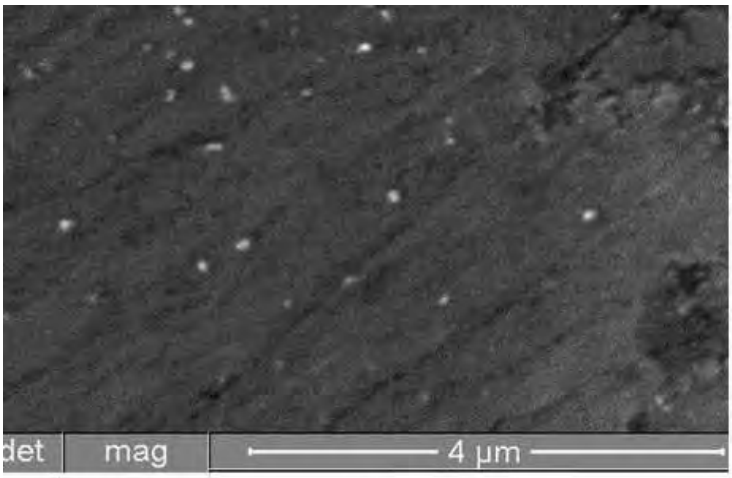

(a)

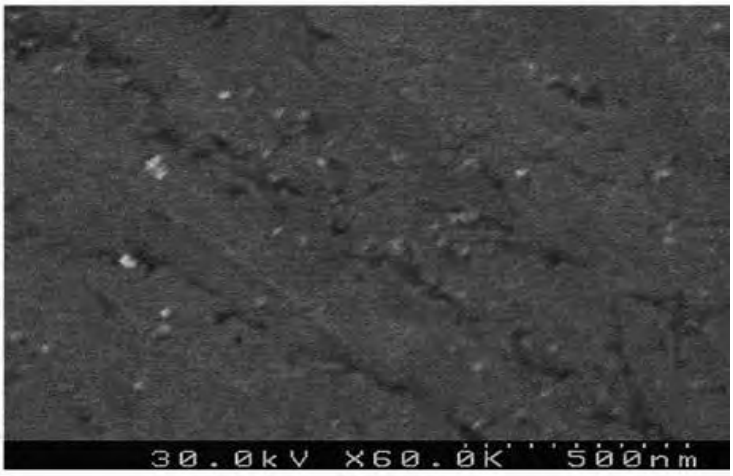

(b)

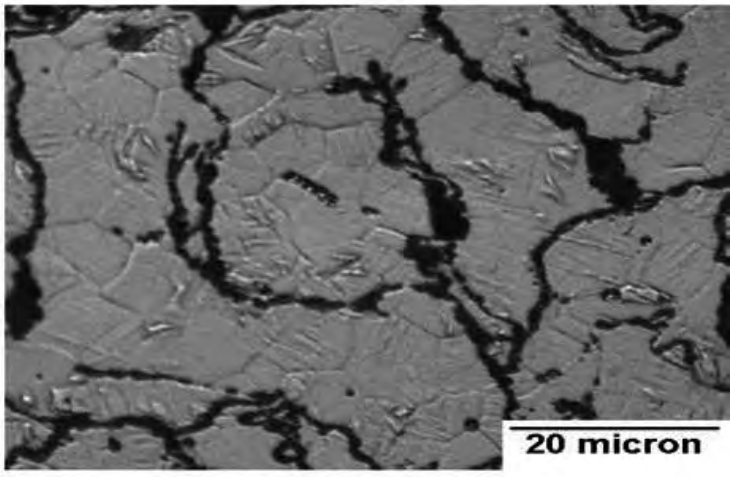

(c)

Figure 1. Representative micrographs showing: (a) and (b) reinforcement distribution of Al_2O_3 and ZrO_2, and (c) typical grain morphology in the case of Mg/ZrO_2, respectively (*5*).

2.2 Melt-based Processing

In the most basic type of melt-based processing, known as stir casting, the desired amount of reinforcements is stirred into molten Mg. Once dispersed, a number of options exist for producing the nanocomposite. The most direct method is to cast the Mg into a mold or die, from which the part is extracted and prepared for use. One aspect of this process that must be mastered is the homogeneous distribution of the nanoreinforcement throughout the Mg matrix. Failure to do so generates matrix-rich or reinforcement-rich regions, which tend to be weaker than the uniformly reinforced matrix. Another issue with stir casting is the entrapment of gases, which can lead to undesired porosity and, hence, a decrease in mechanical performance. Despite these challenges, stir casting is a popular method, as it lends itself easily to large scale production efforts. Indeed, stir casting has been used to produce Mg reinforced with micron-sized SiC particles. To date, however, stir casting has not been routinely used to produce nanoparticle reinforced Mg, as the high specific surface area and low wettability of the nanoparticles in the molten metal makes it extremely challenging to uniformly disperse the nanoparticles in the melt (*21*). Micrographs in figure 2 demonstrate how nanoparticles refine grain structure in cast Mg, even after rolling and a recrystallization heat treatment.

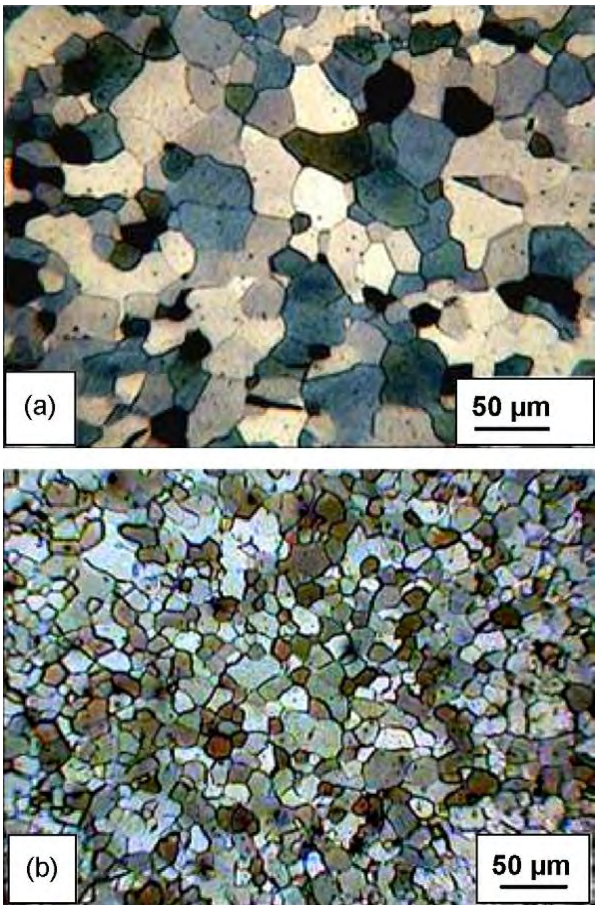

Figure 2. Optical micrographs showing the grain structure of (a) pure Mg and (b) Mg–2Al_2O_3 after hot rolling and full recrystallization heat treatment (*39*).

A variation of conventional stir casting that yields Mg nanocomposites by the conversion of polysilazane pellets to Si-C-N-O nanoparticles in the melt immediately prior to casting has recently been introduced (*22*). In this case, the intention is that the ceramic nanoparticles would retain the state of dispersion achieved by the mixing of the polymeric pellets in the melt prior to pyrolysis. This initial effort revealed that the nanoceramics formed by pyrolysis segregated to the grain boundaries in the cast material; such segregation of nanoreinforcements to grain boundaries during solidification is a relatively common issue for cast materials. Although the initial results were promising, much work remains to be done to achieve the desired microstructure (uniformly dispersed nanoparticles) that will yield the improvements in tensile properties typically observed in other systems described in this report.

In an attempt to overcome the issue of agglomeration in stir casting, an increasingly popular approach is the use of ultrasonic agitation to disperse nanoparticles in the melt prior to casting. It is believed that the ultrasonic cavitation, in combination with local temperatures exceeding 5000 °C, can break apart nanoparticle clusters and clean the particle surfaces (*21, 23*). Much of the initial work using this method is aimed at incorporating SiC nanoparticles into pure Mg. Recently, the concept has been extended to zinc containing alloys, such as AZ91D or a customized Mg-zinc alloy in which three different zinc levels were used: 4, 6, or 8 weight percent (w%) (*24, 25*). Although the nanoparticles, on average, were well-dispersed, some SiC agglomerates on the order of 100–300 nm were observed. Furthermore, elemental analysis indicated that the particles were partly oxidized. Tensile testing indicated a significant increase in strength and ductility for the nanocomposites relative to the monolithic Mg. Although the method does indeed show much promise, the effort of transitioning this technology to large scale production is still being addressed.

Other melt-based processing approaches seek to atomize the molten melt in an effort to ensure a relatively homogeneous distribution of the nanoparticles. The first of these, known as disintegrated melt deposition (DMD), has been widely used to produce Mg nanocomposites (*15, 26–33*). In this approach, nanoceramic powders are added to the Mg melt in a graphite crucible under an inert atmosphere. After stirring to disperse the nanoparticles, the melt is released through an orifice at the bottom of the chamber. Upon exiting, the melt is disintegrated by twin jets of Ar gas orientated normal to the melt stream. The resulting particles are deposited onto a metallic substrate, forming a billet that is subsequently machined to a diameter suitable for extrusion. After a period of isothermal annealing, the ingot is extruded at the desired temperature (typically around 250 °C) to yield 7–8 mm rods suitable for evaluation and testing.

A method closely related to the DMD technique is spray forming, or spray casting (*34, 35*). In this process, the melt proper is delivered into a gas atomizer, where an inert gas (typically Ar) is used to atomize the melt into fine molten droplets, which are collected into a billet. The droplets strike the substrate in the semi-solid state, thereby providing enough liquid fraction to hold the solid fraction in place. The rapid cooling that occurs in the spray results in fine, equiaxed microstructures on the order of 10–100 μm. Moreover, spray forming can be used to produce

material in strip, tube, ring, or bar form, often while reducing the number of processing steps between the melt and finished product. However, two major issues hinder the widespread use of spray casting. First is the relatively low process yield, approximately 75%, that results from the overspray of the powder that misses the collection substrate. The ability to collect the overspray powder and re-inject it or sell it is helping to reduce the negative influence of this issue on the process. The second issue is the lack of precise process control due to the highly complex nature of the process. This lack of process control complicates the production of composite materials with repeatable properties.

Although brief, this section has identified many of the processing methods commonly used to manufacture Mg reinforced with various types of nanoparticles. As could be expected, the methods associated with the production of monolithic Mg (be it pure or alloyed) are the most developed. That said, many of the newer methods offer the potential for producing Mg nanocomposites with uniformly dispersed nanoparticles.

3. Selected Review of Nanocomposite Properties

This section will discuss the influence that the addition of nanosized reinforcements has on the properties of Mg. The majority of work to date has focused on grain size refinement, tensile properties, and microhardness, with limited work done in areas such as wear and oxidation resistance. A general overview of the influence that nanoparticle type and volume fraction have on selected material properties will be presented.

3.1 Grain Size

Microstructural examination of nanoreinforced Mg indicates that the grains are typically equiaxed and reduced in size relative to monolithic Mg. This effect of the nanoparticles on the microstructure has typically been attributed to two factors. First, the nanoparticles act as nucleation sites for Mg grains during recrystallization. Second, the nanoparticles act to pin grain boundaries, thereby restricting the amount of grain growth that can occur during recrystallization.

Obviously, the degree to which the nanoparticles are uniformly dispersed in the Mg matrix will determine how effective they are in refining grain size and structure. Indeed, research by Hassan and Gupta demonstrates this important truth. For example, in nanocomposites of commercially pure Mg and 50 nm alumina particulates produced by the BPS method, a significant reduction in grain size was not observed until approximately 1.1 volume percent (v%) of particulates were added (*4*). In contrast, grain size in nanocomposites produced by DMD dropped significantly—from 49 to 6 μm—upon the introduction of nanoparticles and then appeared to be insensitive to reinforcement content (0.7, 1.1, or 2.5 v%) (*27*). The significant difference in grain refining ability between the two processing methods is shown in table 1, and was attributed to the

reasonably uniform distribution of the nanoparticles achieved by the vigorous stirring of the slurry prior to disintegration and deposition that occurs in the DMD process (in comparison to the relatively ―static" nature of the powder metallurgy approach) (*15*).

Table 1. Influence of processing method on grain size and tensile properties for alumina reinforced Mg. BPS data from (*4*). DMD data from (*28*).

Material	Grain Size (μm)	0.2% Yield Strength (MPa)	Ultimate Tensile Strength (MPa)	Ductility (%)
Blend-Press-Sinter				
Mg	60 ± 10	132 ± 7	193 ± 2	4.2 ± 0.1
Mg/0.66v% Al_2O_3	63 ± 16	191 ± 2	247 ± 2	8.8 ± 1.6
Mg/1.11v% Al_2O_3	31 ± 13	194 ± 5	250 ± 3	6.9 ± 1.0
Directed Melt Deposition				
Mg	49 ± 8	97 ± 2	173 ± 1	7.4 ± 0.2
Mg/0.7v% Al_2O_3	6 ± 2	214 ± 4	261 ± 5	12.5 ± 1.8
Mg/1.1v% Al_2O_3	6 ± 1	200 ± 1	256 ± 1	8.6 ± 1.1
Mg/2.5v% Al2O3	4 ± 1	222 ± 2	281 ± 5	4.5 ± 0.5

Although the previous example illustrated the influence of processing method on grain size, experimental observations in this regard can often be inconsistent or contradictory. For yttria nanocomposites processed using a powder metallurgy technique, followed by microwave sintering and extrusion, essentially no change in grain size was observed until the reinforcement content reached 0.7 v% (*11*). Yet, observations from a subsequent study on the effect of extrusion ratio revealed no difference in grain size between pure Mg and nanocomposites, with 0.7 v% Y_2O_3 processed using the same extrusion ratio (*12*). Goh et al. observed a progressive reduction in grain size in their study on Mg containing 0.5, 1.0, and 2.0 v% of nanosized yttria particles processed by DMD/extrusion (*36*). However, measurements by Hassan and Gupta on nanocomposites formed by BPS/extrusion showed an apparent maximum in grain size reduction for yttria nanocomposites. In this study, the grain size was reduced from 60 μm to 25 μm for 0.22 v% yttria, which then leveled off at 13 μm for 0.66 and 1.11 v% (*10*). This upper limit was attributed to the inability of powder-based processing to break up the particle clusters typically observed at higher reinforcement levels. At this time, this seemingly disparate relationship between grain size and reinforcement content for Mg/yttria nanocomposites has not been fully explained or addressed in a thorough study.

While studies indicate that the addition of virtually any nanosized reinforcement will achieve some degree of grain refinement, experimental results seemingly indicate that some reinforcements are more effective than others in achieving microstructural refinement. The results from one study on grain size in Mg containing 1.1 v% of Al_2O_3, Y_2O_3, or ZrO_2 are shown in table 2. Experimental results indicated that yttria and zirconia were more effective than alumina in reducing grain size (*5*). The authors attribute this trend to the higher thermal stability

of both yttria and zirconia, compared to alumina, in Mg. To date, it does not appear that this effort has been repeated or expanded to other reinforcement types.

Table 2. Influence of reinforcement type on grain size and tensile properties (*5*).

Material	Grain size (μm)	0.2% Yield Strength (MPa)	Ultimate Tensile Strength (MPa)	Ductility (%)
Mg	60 ± 10	132 ± 7	193 ± 2	4.2 ± 0.1
Mg/1.1v% Al_2O_3	31 ± 13	194 ± 5	250 ± 3	6.9 ± 1.0
Mg/1.1v% Y_2O_3	12 ± 3	153 ± 3	195 ± 2	9.1 ±0.2
Mg/1.1v% ZrO_2	11 ± 3	146 ± 1	199 ± 5	10.8 ± 1.3

Similarly, there has only been minimal effort at determining the effect of reinforcement size on grain refinement. In their study on elemental Mg reinforced with three different sizes of alumina particles (1.0 μm, 0.3 μm, and 50 nm), Hassan and Gupta determined that the addition of the larger particles actually resulted in a smaller grain size than that found in the composite with nanosized reinforcements (table 3) (*26*). This observation was attributed to the comparatively higher tendency of the nanosized particles to form clusters than the micron-sized particles.

Table 3. Strength improvement relative to pure Mg and commercial viability for several processing methods used to produce nanocomposites. Commercial viability is adapted from (*47*).

		Commercial viability		
Process Method	**Strength Improvement**	**Lot size**	**Compatibility with infrastructure**	**Range of product forms**
Blend-Press-Sinter	++	+	++	+
Microwave Sintering	+	+	+	+
Extrusion	+ only for highest ratio or low temperatures (< 150 °C)	++	+++	+
Directed Melt Deposition	+++	++	++	++

Within the last few years, researchers have branched out from ceramic reinforcements to the use of nanosized metallic, or a combination of metallic and ceramic, reinforcements. Wong and Gupta have published results for pure Mg containing 0.3, 0.6, or 1 v% Cu nanoparticles (~50 nm) by the microwave sintering of billets of blended Mg/Cu powders (*20*). After sintering, the billets were extruded at 350 °C using a ratio of 25:1.

Microstructural analysis indicated that nanosized Cu particles, as well as the reaction product Mg_2Cu, were located along the Mg grain boundaries. The grains were typically equiaxed, with a grain size reduction from 27 μm for the monolithic matrix to approximately 15 μm for the

nanocomposites. Recently, Tun and Gupta have created a hybrid nanocomposite by adding nanosized yttria (30–50 nm) and Ni (20 nm) to pure Mg (*19*). The yttria content was held constant at 0.7 v%, while the nickel content varied from 0.3, 0.6, or 1.0 v%. Microstructural analysis indicated that yttria, by itself, did not result in a significant change in grain size. However, upon the addition of 0.3 v% nickel nanoparticles, the grain size was reduced from 18 μm to 9 μm. This sizeable reduction in grain size was attributed to the formation of Mg_2Ni intermetallic phases during processing. Further increasing the nickel content did not result in a demonstrable effect on grain size.

3.2 Microhardness and Wear Resistance

As expected, the incorporation of nanosized ceramic reinforcements into Mg resulted in a higher microhardness than monolithic Mg. For example, Lan et al. observed a linear relationship between microhardness and SiC content (0–5 w%) for AZ91D/SiC nanocomposites (*37*). Relative to the nonreinforced alloy, AZ91D with 5 w% SiC displayed a 75% increase in microhardness. This improvement was attributed to a uniform dispersion of the SiC nanoparticles in the Mg matrix. Similar results have been observed in the majority of other nanocomposite systems. In general, improvements in microhardness were attributed to the presence of the harder ceramic particles, the smaller grain sizes in the nanocomposite, and the constraint imposed on matrix deformation by the presence of the nanoparticles.

Similarly, improvements have also been observed for the wear resistance of Mg nanocomposites. Lim et al. examined the wear resistance of CP Mg containing up to 1.1 v% of 50 nm alumina particulates using a 10 N load and sliding speeds up to 10 m/s (*31*). Test results, shown in figure 3, indicated that all nanocomposites showed a reduction in wear rate relative to the base alloy, with the 1.11 v% composite showing the highest reduction. For all samples, the wear rate decreased up to a speed of 7 m/s, with abrasion and adhesion being the primary wear mechanisms. Above this speed, the wear rate increased due to an increase in frictional heating between the pin and sample that caused a transition to wear by thermal softening. Within the last year, wear testing has been performed on pure Mg and AZ31 reinforced with 2 w% of 100 nm alumina particles (*38*). Wear tests were conducted using speeds of 0.5 or 1.5 m/s, with normal loads of 12, 24, and 36 N (equivalent to 0.5, 1.0, and 1.5 MPa, respectively). For all conditions, the nanocomposites had superior wear resistance and higher work-hardening rates relative to non-reinforced materials. The improvement in wear resistance for the nanocomposites in both studies was attributed to the presence of the harder particles that resulted in grain refinement and load transfer from the matrix to the harder alumina particles.

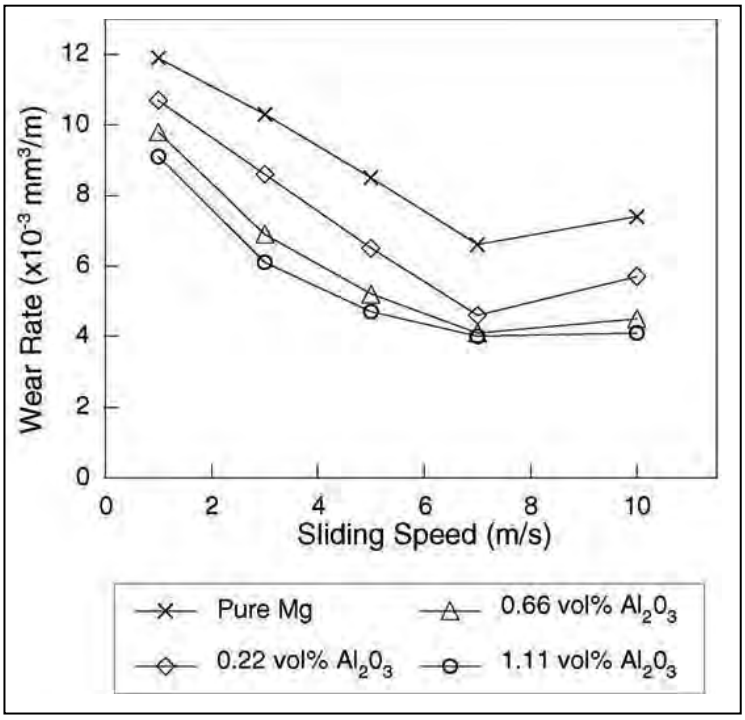

Figure 3. Pin on disk wear rate for a 10 N as a function of sliding speed f or pure Mg and alumina nanoreinforced Mg (*31*).

3.3 Tensile Properties

It has been well-established that the incorporation of second phases, such as micron-sized whiskers or particulates, results in improved mechanical properties relative to the monolithic matrix material. Thus, it is not surprising that significant improvements in tensile properties (0.2% yield strength, ultimate tensile strength) have been observed in nanoreinforced Mg. Somewhat surprising, however, is the sizeable increase in tensile ductility that has been observed in many of the Mg nanocomposites reviewed for this survey. This section will summarize the explanations for the observed property improvements, as well as illustrate how tensile properties are influenced by reinforcement type or processing methods.

3.3.1 Strength

In seeking to explain the improved strengths of nanoreinforced Mg, researchers have identified four potential factors that contribute to the observed behavior (*36, 39*). Given the finer grain size commonly seen in the nanocomposites, there is an increase in strength associated with dislocations piling up at grain boundaries, known as the Hall-Petch effect. Next, dislocation motion may also be impeded by the presence of the nanoparticles. This interaction between dislocations and nanoparticles is known as Orowan strengthening, and is dependent on the diameter and spacing of the nanoparticles. A third factor that contributes to increased strength in the nanocomposites is the generation of thermally induced residual stresses and geometrically necessary dislocations due to the difference in thermal expansion coefficients of the

nanoparticles and Mg matrix. The final factor is that of load transfer by shear from the soft matrix to the hard nanoparticles during tensile testing. By definition, this contribution assumes a strong interface between the nanoparticles and the matrix, and is dependent on the volume fraction of the nanoparticles and the yield strength of the matrix. Analysis of these strengthening mechanisms has indicated that CTE mismatch and Orowan strengthening are the two primary contributors, followed by Hall-Petch and load transfer (*39–41*).

3.3.2 Elongation/Ductility

With regard to elongation, the majority of researchers have also reported an increase in tensile ductility in nanoreinforced Mg relative to the monolithic alloy. Certainly, a key aspect of this ductility increase is the refined grain structure found in the nanocomposites since the ductility of pure Mg increases appreciably as the grain size is refined (*42–43*). Furthermore, in contrast to the case of ductile matrices, it has been shown that the hard nanoparticles have a beneficial role in the brittle HCP matrix. The presence of the dispersed nanoparticles acts to provide sites where cleavage cracks may open in front of the advancing crack to dissipate stress concentrations at or near the crack front; the dispersion also effects a change in the stress state from plane strain to plane stress near the crack tip (*44*). Moreover, it has been observed that the presence of the nanoparticles allows non-basal slip systems to become active during axial tensile loading (*10*). Finally, in certain Mg alloys, the presence of ceramic nanoparticles has been shown to reduce the size and sharpness of second phases. For example, experiments conducted on nanoreinforced AZ31 indicated up to a 113% increase in tensile failure strain for AZ31 reinforced with 1.5 volume percent alumina (*33*). Microstructural analysis revealed that the presence of nanoparticles reduced the size and sharpness of the intermetallic β–$Al_{12}Mg_{17}$ phase, thereby reducing the amount of localized stress buildup around the intermetallic particles (*29, 33*).

3.3.3 Influence of Processing Method

Tensile testing indicated that the degree of improvement in tensile properties was dependent on the processing method used in producing the material (tables 1 and 3) (*4, 15, 28*). For example, elemental Mg nanocomposites produced by the BPS method showed up to a 50% increase in tensile yield strength and 30% increase in tensile ultimate strength relative to monolithic Mg (*4*). The property improvement in the DMD nanocomposites was much more dramatic — up to 129% improvement in tensile yield strength and 62% improvement in ultimate tensile strength for CP Mg (*28*). More modest improvements were observed in the case of the alloy AZ31—19% increase in tensile yield strength and 21% in ultimate tensile strength (*33*). Microstructural analysis indicated that samples produced by DMD had a finer grain size than those produced using powder metallurgy, an observation attributed to the uniform distribution of the nanoparticles in the DMD method (*4, 15, 28*). The smaller grain size contributes to the increased strength through increased frequency of dislocations piling up at grain boundaries, whereas the uniform dispersion of nanoparticles in the DMD material would be more effective at pinning dislocations.

Tun and Gupta have used microwave sintering to produce Mg nanocomposites containing 0.5 or 2.0 w% yttria (*12*). Microscopy on the extruded samples indicated that the addition of yttria had essentially no influence on grain size. Tensile testing indicated a progressive increase in tensile yield strength (7.5% for 0.5v% and 17% for 2.0v%) and ultimate tensile strength (11% for 0.5v% and 26% for 2.0). However, the ductility for the nanocomposites is unchanged relative to the monolithic Mg. A later study on the influence of heating rate used for the microwave-sintering of the nanocomposite showed that the mechanical properties of the samples produced using the lower heating rate (20 °C/min) were inferior to those samples produced with a heating rate of 49 °C/min (*18*). Indeed, the properties obtained from the lower heating rate samples were lower than that of unreinforced Mg. The poor performance of the samples heated at the lower rate was attributed to poorly distributed particulates with regions of clusters and/or agglomerates, as well as larger pores along the particle/grain boundary regions.

Tun and Gupta have also examined the influence of extrusion ratio on the mechanical properties of pure Mg containing 0.7 v% yttria nanoparticles (size – 30–50 nm) (*12*). In this study, nanocomposites were blended, pressed, and then microwave-sintered to near full density. Representative micrographs from billets extruded at 350 °C using extrusion ratios of 12:1, 19:1, or 25:1 are shown in figure 4. Results from these experiments are detailed in figure 5, which shows that the strength (yield, ultimate) of the reinforced material was greater than that of pure Mg only for the highest extrusion ratio. A similar pattern was observed for the strain to failure. These trends were attributed to the presence of particulate clusters in the matrix, which degrade the performance of the nanocomposite. These clusters remained intact until a sufficiently high enough extrusion ratio was used, which broke down the clusters and achieved a more uniform distribution of the yttria nanoparticles.

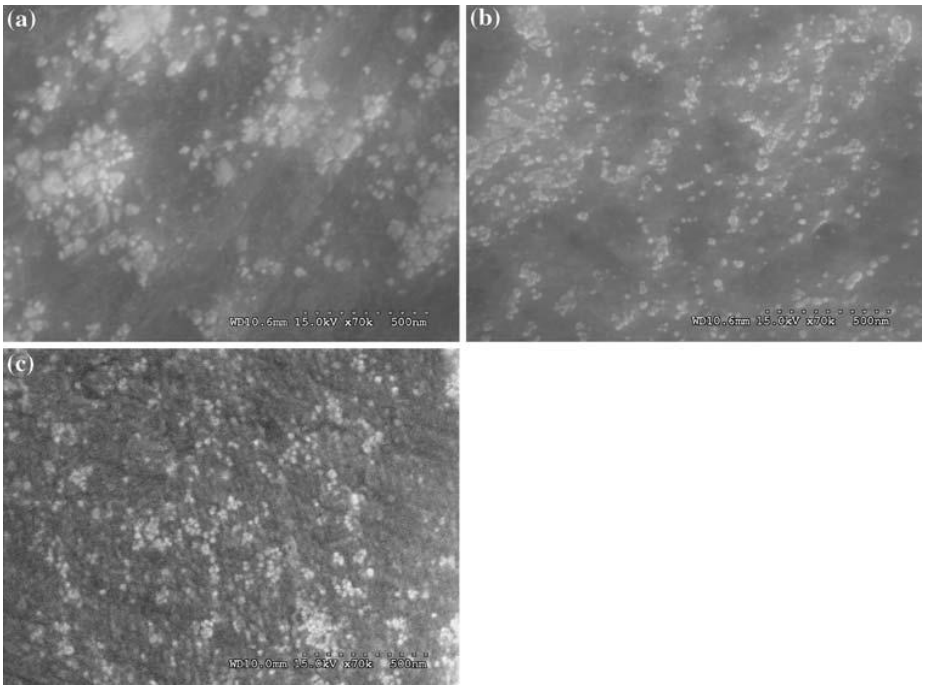

Figure 4. FESEM micrographs showing particle distribution in Mg/Y_2O_3 nanocomposites extruded at extrusion ratio of (a) 12:1, (b) 19:1, and (c) 25:1 (*12*).

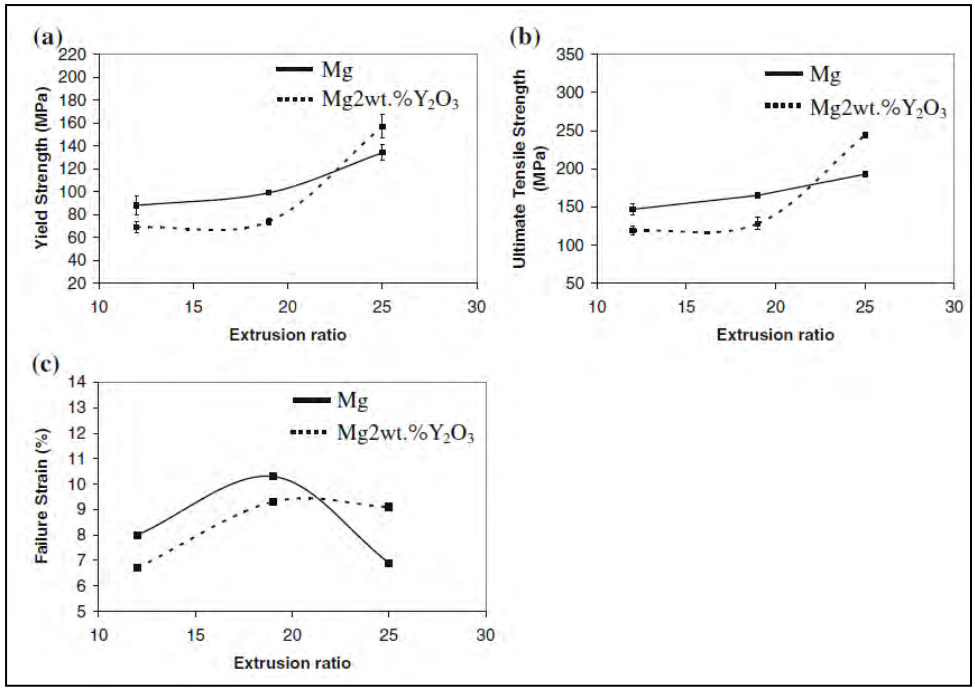

Figure 5. Influence of extrusion ratio on the tensile properties of Mg/0.7v% (2w%) Y_2O_3 nanocomposites (*12*).

Lim and Gupta studied the influence of extrusion temperature (350, 250, 150, or 100 °C) on the microstructure and mechanical performance of a 11.5 wt% (6.6 v%) SiC/Mg nanocomposite (*45*). Microstructural examination revealed that reducing the extrusion temperature reduced the number of particulate clusters, as well as the average grain size. As a result, composites extruded at the lower temperatures (100, 150 °C) displayed the greatest improvement in hardness, modulus, and 0.2% yield strength. The ultimate tensile strength and failure strain were essentially constant (~200 MPa and 3.5%, respectively) over the range of extrusion temperatures used in the study.

Ugandhar et al. investigated the influence of a recrystallization heat treatment on the strength and ductility of Mg reinforced with either 2.7 or 9.0 v% of submicron (0.6 μm) SiC particles (*46*). Tensile test results indicated that the composite with the higher SiC content had poorer tensile properties. This behavior was attributed to a reduced cavitation resistance resulting from the higher porosity and particulate content. Results from tensile tests indicated that the recrystallized (150 °C/5 hours) samples had improved yield strength, ultimate strength, and ductility relative to the as-extruded samples. This improvement was attributed to stress relief at the matrix/particulate interface.

3.3.4 Influence of Reinforcement

As seen in table 2, the addition of 1.1 v% ceramic nanoparticles resulted in sizeable increases in tensile properties relative to pure Mg (*5*). However, it is clear that the degree of property improvement was dependent on particle type. For example, alumina-reinforced Mg shows the highest strength values due to the formation of high strength interfacial bonds between the alumina nanoparticles and the Mg matrix. In contrast, zirconia-reinforced Mg had the highest ductility increase, accompanied by marginal improvements in strength. As a result, Mg/zirconia nanocomposites had the highest energy absorbing ability (as determined by the calculated work of fracture). Thus, it was concluded that Mg/alumina nanocomposites were best suited for strength-critical designs, whereas Mg/zirconia nanocomposites were best suited for those requiring damage tolerance (*5*).

3.3.4.1 Alumina

Experimental results on tensile properties generally indicate that the addition of alumina, up to approximately 1.1 v%, resulted in a progressive increase in tensile properties (modulus, 0.2% yield and ultimate strength, ductility) (*4, 28*). Increasing the alumina content to 2.5 v% further increased the modulus and strength, but at the cost of lowering ductility below that of monolithic Mg—a pattern also observed in pure Mg reinforced with nanosized (29–68 nm) zirconia particles (*44*). For both reinforcements, a volume fraction of 0.66% produced the nanocomposite with the best combination of strength and ductility, as indicated by the highest value for work of fracture.

Experimental observations also indicate a relationship between tensile properties and the size of the Al_2O_3 particulates (*26*). As shown in table 4, improvements in hardness and strength values

were achieved with both nano- and micron-sized reinforcements. However, ductility and work of fracture improvements were only significant for the nanoreinforced reinforcements. In comparison, the ductility of the Mg reinforced with micron-sized particulates decreased by more than 50% relative to the monolithic alloy. Finally, an examination of the fracture surfaces indicated a change in fracture behavior from a complete cleavage mode for the monolithic alloy to a mixed mode of ductile and intergranular fracture for nanoreinforced material.

Table 4. Influence of reinforcement size on various properties in a Mg/Al_2O_3 nanocomposite. The data for AZ91/SiCp is shown for comparison (*26*).

Material	Grain size (μm)	0.2% Yield Strength (MPa)	Ultimate Tensile Strength (MPa)	Ductility (%)	Macrohardness (15 HRT)	Microhardness (HV)	Work of Fracture (J/m^3)
Mg	49 ± 8	97 ± 2	173 ± 1	7.4 ± 0.2	37.1 ± 0.7	40.0 ± 0.2	11.1 ± 0.3
Mg/Al_2O_3 (50 nm)	14 ± 2	175 ± 3	246 ± 3	14.0 ± 2.4	64.6 ± 0.8	65.9 ± 0.9	31.7 ± 6.3
Mg/Al_2O_3 (0.3 μm)	6 ± 1	200 ± 1	256 ± 1	8.6 ± 1.1	59.4 ± 0.6	52.0 ± 0.8	20.9 ± 2.8
Mg/Al_2O_3 (1.0 μm)	5 ± 1	209 ± 1	242 ± 3	3.5 ± 0.3	63.8 ± 0.5	58.8 ± 0.5	7.0 ± 0.9
AZ91/9.3% SiCp	-	120 ± 5	181 ± 6	4.7 ± 1.3	-	-	8.8 ± 2.0

3.3.4.2 Yttria

In contrast to the continual increase in strength observed for alumina-reinforced Mg, the dependence of strength on reinforcement content in yttria-reinforced Mg was markedly different. For example, Hassan and Gupta observed that yield strength was essentially constant for nanocomposites containing 0.22, 0.66, or 1.11 v% yttria (~153 vs. 132 MPa for pure Mg) (*10*). In contrast, the ultimate strength showed only a marginal increase relative to pure Mg (193 MPa), and actually decreased with increasing yttria content, from 211 MPa at 0.22 v% to 195 MPa at 1.11 v%. This trend in properties was attributed to an increase in porosity and reinforcement clustering with increasing reinforcement content (*10*). While strength was only moderately improved in the nanocomposites, there was a significant increase in ductility of the nanocomposites relative to pure Mg (an increase up to 15.8% from 4.2% for pure Mg). However, sample ductility showed an inverse relationship with reinforcement content, from a maximum of 15.8% for 0.22 v% to 9.1% for 1.11 v%. This combination of property trends resulted in the maximum work of fracture occurring for a volume content of 0.22%.

3.3.4.3 Copper

In a recent study, Wong and Gupta examined the tensile properties of pure Mg containing 0.3, 0.6, or 1v% Cu nanoparticles (~50 nm) (*20*). The extruded nanocomposites had an equiaxed grain structure with the Cu nanoparticles, as well as the reaction product Mg_2Cu located along the grain boundaries. Tensile testing showed that the yield and ultimate strength reached their maximum value for the 0.6 v% nanocomposite, and then decreased when the reinforcement content was raised to 1.0 v%. In contrast, the failure strain steadily decreased from a value of 6.1% for the monolithic matrix down to 2.9% for the 1.0 v% nanocomposite. The decrease in tensile properties with higher Cu content, as well as the continual reduction in ductility, was attributed to the increasing amount of the harder Cu reinforcement and the brittle Mg_2Cu intermetallic phases. It is believed that agglomerates formed from Cu nanoparticles or the intermetallic phase led to grain boundary embrittlement, as well as serving as sites for potential crack initiation. Despite the progressive decrease in ductility with reinforcement content, these nanocomposites may hold promise, as Mg/Cu nanocomposites generally had higher specific modulus and strength than Mg reinforced with higher volume fraction of micron-sized reinforcements, as well as Mg reinforced with ceramic nanoparticles.

3.3.4.4 Hybrid Nanocomposites

Recently, Tun and Gupta created a hybrid nanocomposite by adding nanosized yttria (30–50 nm) and nickel (20 nm) to pure Mg (*19*). The yttria content was held constant at 0.7 v%, while the nickel content varied from 0.3, 0.6, or 1.0 v%. Mechanical testing indicated that both yield strength and ultimate tensile strength increased with the addition of 0.3 and 0.6 v% nickel. There was essentially no difference in strength values for the 0.6 and 1.0% nickel nanocomposites. In contrast, failure strain was improved by approximately 30% (from 7% to 9%) for nanocomposites up to 0.6% nickel. However, increased clustering of the intermetallic phase Mg_2Ni for the 1.0 v% nickel nanocomposite resulted in a reduction of the failure strain to 5.5%.

Thakur et al. have produced Mg nanocomposites reinforced with 40–70 nm sized multi-wall carbon nanotubes (CNT), as well as a combination of CNT and Al_2O_3 nanoparticles (*48*). The total reinforcement content was kept constant at 1 w%, using either all CNT or a combination of CNT and nanoparticles (see table 5). Samples were produced using the BPS/extrusion method. Poor interfacial bonding, as well as an uneven distribution and tendency for the CNT to agglomerate, were cited as reasons for the poor tensile performance of the CNT-only nanocomposite. However, an increase in the Al_2O_3 content accompanied by a reduced CNT content resulted in progressive increases in both yield strength and ultimate tensile strength. In contrast, the failure strain showed a marginal increase following the initial introduction of Al_2O_3 and remained essentially constant over all alumina content. This behavior was attributed to the higher degree of grain refinement in the alumina nanocomposites, as well as the stronger interfacial bonding between the alumina nanoparticles and the Mg matrix.

Table 5. Tensile properties of hybrid CNT/Al_2O_3 nanoparticle reinforced Mg from (*48*). Extruded pure Mg properties from (*47*).

Material	0.2% Yield Strength (MPa)	Ultimate Tensile Strength (MPa)	Ductility (%)
Pure Mg, extruded	69–105	165–205	
Mg/1w% CNT	112.9 ± 2.8	146.5 ± 6.5	1.9 ± 0.9
Mg/0.7w% CNT/0.3w% Al_2O_3	131.4 ± 6.2	164.3 ± 11.2	2.6 ± 1.3
Mg/0.5w% CNT/0.5w% Al_2O_3	136.5 ± 5.8	181.0 ± 8.6	2.5 ± 0.4
Mg/0.3w% CNT/0.7w% Al_2O_3	153.5 ± 2.1	196.0 ± 3.3	2.5 ± 0.8

Nguyen and Gupta have examined the tensile properties of AZ31B reinforced with either Cu or a combination of alumina and Cu nanoparticles (*49*). Tensile testing of samples produced using DMD/extrusion indicated that yield and ultimate strengths generally increased with reinforcement content (see table 6). However, the relationship between failure strain and reinforcement content was mixed. For AZ31B/Cu nanocomposites, increasing reinforcement content resulted in a decrease in ductility. This was most noticeable for the nanocomposite containing 18 w% Cu, which had a failure strain of 1.1% compared to 5.6% for pure AZ31B. However, for both Cu levels, the addition of 3.3w % Al_2O_3 nanoparticles essentially restored ductility values to that of pure AZ31B. Microstructural analysis indicated that the hybrid nanocomposites had a smaller grain size than the AZ31B/Cu nanocomposites. As presented earlier, smaller grains lead to increased strengths and ductility in Mg.

Table 6. Tensile properties of AZ31B reinforced with either Cu or a combination of Cu and alumina nanoparticles (*49*).

Materials	0.2% Yield Strength (MPa)	Ultimate Tensile Strength (MPa)	Ductility (%)
Pure AZ31B	201 ± 7	270 ± 6	5.6 ± 1.4
AZ31B/10w% Cu	240 ± 3	302 ± 2	3.8 ± 0.5
AZ31B/10w% Cu/3.3w% Al_2O_3	241 ± 8	313 ± 9	5.6 ± 0.5
AZ31B/18w% Cu	268 ± 4	310 ± 5	1.1 ± 0.4
AZ31B/18w% Cu/3.3w% Al_2O_3	294 ± 12	344 ± 7	4.8 ± 0.4

3.4 Compressive Properties

In contrast to tensile properties, much less work has examined the compressive properties of nanoreinforced Mg (*3, 22, 30, 33, 50–52*). In each of these studies, the reinforced nanocomposites displayed improved compressive properties relative to the monolithic Mg matrix. For example, Sudarshan et al. reported an approximate 90% increase in yield strength and a 30% increase in ultimate strength for pure Mg strengthened by Si-C-O-N nanoparticles (*22*). However, the extent of the improvement is not consistent for similar nanocomposite

systems. For example, two studies on AZ31B with 1.5v% Al_2O_3 showed significant differences in properties. In both studies, the nanocomposites were fabricated by DMD, followed by hot extrusion at 350 °C. Results from the first study by Nguyen and Gupta, shown in table 7, indicated an approximate 32% increase in yield strength, a 10% increase in ultimate strength, and 13% increase in failure strain (*30*). In contrast, Paramsothy et al. found only a 5% increase in yield and ultimate strength and a minor (~4%) reduction in the average failure strain (*33*). The reason for this significant difference is unknown.

Table 7. Improvement in compression properties for alloy AZ31B with indicated reinforcement content (*30, 51*).

Material	0.2% Yield Strength (MPa)	Ultimate Compressive Strength (MPa)	Ductility (%)
AZ31B	133 ± 4	444 ± 10	12.6 ± 1.0
AZ31B/0.66v% Al_2O_3	172 ± 17	468 ± 10	13.4 ± 1.8
AZ31B/1.1v% Al_2O_3	174 ± 2	478 ± 11	13.5 ± 0.8
AZ31B/1.5v% Al_2O_3	176 ± 7	486 ± 5	14.3 ± 1.2
AZ31B/10w% Cu/3.3w% Al_2O_3	235 ± 8	530 ± 10	10.7 ± 1.5
AZ31B/18w% Cu/3.3w% Al_2O_3	260 ± 12	550 ± 13	9.8 ± 1.9

Recently, Nguyen and Gupta have investigated the influence of micron-sized (8–11 μm average) Cu particles on the compressive response of AZ31B reinforced with Al_2O_3 nanoparticles (*51*). The alumina content was maintained at 3.3 w%, while the Cu content was either 10 or 18 w%. As shown in table 7, experimental results indicated a significant increase in yield and ultimate strength, with only a small decrease in failure strain, following the addition of the Cu nanoparticles. The changes in properties were attributed to the formation of second phases, such as Mg_2Cu and MgAlCu.

In addition to the mechanisms responsible for increased tensile properties, it has been suggested that the formation of twins during compressive deformation can also play a significant role in accounting for the observed property improvements (*30, 50*). The twins formed during compressive deformation act in a similar fashion as grain boundaries by impeding dislocation motion. Twinning also results in a lattice reorientation that is not conducive to basal slip (*50*). Finally, the transformation of dislocations as they pass across the twinning boundary can result in an increased hardening rate within the twin (*50*).

3.5 High Temperature Properties

Although not as extensively investigated, results obtained to date show equally dramatic improvements in the elevated temperature response of Mg nanocomposites. Shown in figure 6 are the room temperature and elevated temperature results for elemental Mg containing 1.1 v% Al_2O_3 nanoparticles (*32*). Test results indicated that the nanocomposite retained a high

percentage of its strength up to 150 °C; however, significant strength reduction occurred when tested at 200 °C. Although a slight strength loss was observed at 150 °C, the tensile properties of the Mg/1.1 v% Al_2O_3 nanocomposite exceeded the room temperature strength of monolithic Mg, as well as Mg reinforced with 9.3v% SiC particulates (see table 8) (*32*). In addition, the nanocomposite displayed an approximate 600% increase in ductility, reaching failure strains of 45% at both 150 and 200 °C.

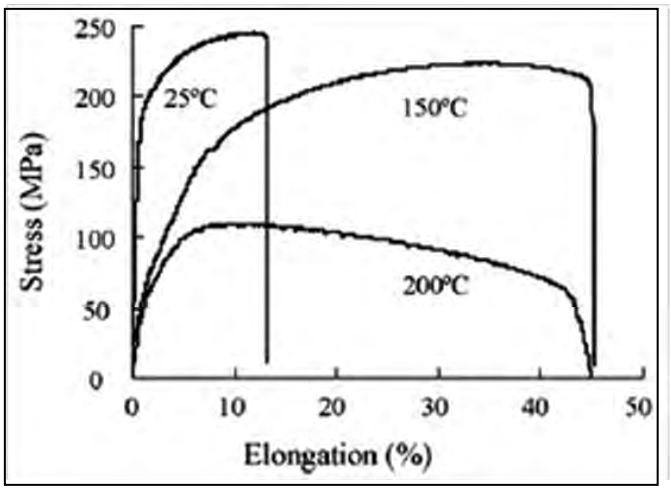

Figure 6. Elevated temperature properties of Mg/1.1v% Al_2O_3 nanocomposites (*32*)

Table 8. Tensile properties as a function of temperature for pure Mg, a nanocomposite with 1.11v% Al_2O_3, and a particulate composite with 9.3v% SiC (*32*).

Material	Test Temperature	0.2% Yield Strength (MPa)	Ultimate Tensile Strength (MPa)	Ductility (%)
Mg	RT	97	173	7.4
	RT	175	246	14.0
Mg/1.11v% Al_2O_3	150 °C	162	224	45.0
	200 °C	95	110	44.7
Mg/9.3v% SiC_p	RT	120	181	4.7

Prasad et al. performed a series of compression tests on pure Mg containing 1 v% Al_2O_3 at elevated temperatures and strain rates in order to determine the hot workability of the material (*14*). Their test results revealed that the nanocomposite had a higher flow stress than the monolithic Mg over the entire test program, especially at lower strain rates.

The reduced rate of deformation has also been observed in compressive creep tests. In an initial round of experiments, Sudarshan et al. observed that pure Mg reinforced with approximately 3w% Si-C-N-O nanoparticles (100–200 nm) possessed steady-state creep rates in compression that were 1–2 orders of magnitude lower than pure Mg for a test temperature of 450 °C (*22*). In figure 7, the open symbols represent data obtained from pure Mg, while closed symbols represent data obtained from the Mg nanocomposites. They assert that this improvement is less than could be anticipated in a nanocomposite with uniformly dispersed nanoparticles.

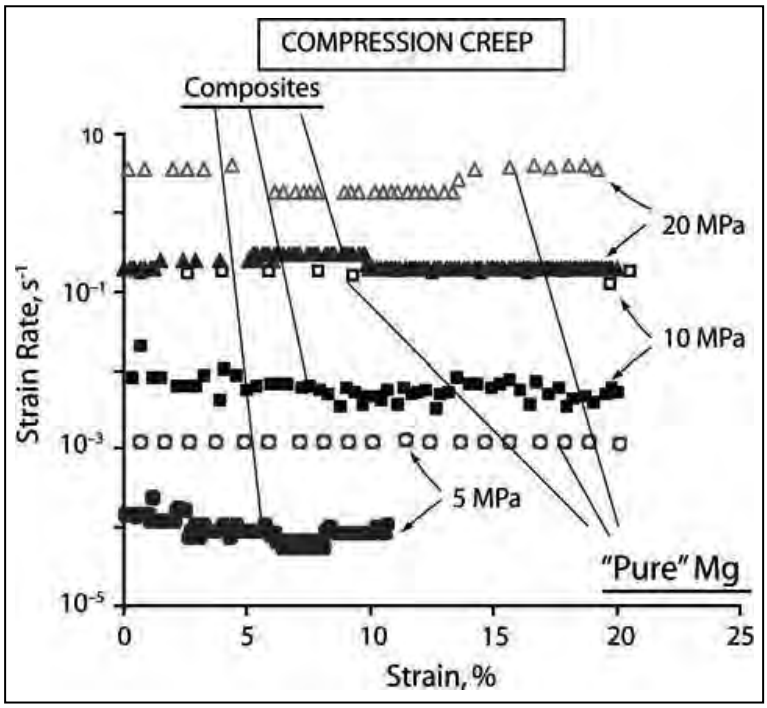

Figure 7. Compression creep rates for pure Mg and nanocomposites containing approximately 3v% Si-C-N-O nanoparticles (*22*).

In more detailed creep studies on yttria-reinforced Mg, researchers have shown that a threshold stress, approximately 30 MPa, exists at which point the creep response of the nanocomposites changes dramatically (*8, 53*). Below this stress level, the nanocomposites are characterized by low creep rates, a low sensitivity to stress (as indicated by apparent stress exponent), and a low sensitivity to temperature (*53*). Above this threshold stress, the nanocomposites show a rapid increase in steady-state creep rate and a much higher stress exponent.

In their work on pure Mg reinforced with 5 v% of 6-micron Y_2O_3 particles, Garcés et al. found that the creep resistance of unreinforced Mg was superior to that of the nanocomposite at temperatures less than 300 °C (*8*). This behavior was attributed to the strong texture present in the monolithic Mg, which was a stronger barrier to dislocation slip than the nanoparticles in the composite. At test temperatures above 300 °C, additional slip systems become operational in the unreinforced Mg and, as a result, the creep resistance of the nanocomposite becomes superior to that of the pure metal.

In contrast to a temperature-dependent response, Han and Dunand have separated the response of Mg reinforced with 30 v% yttria (330 nm size) into low (<30 MPa) and high stress (>34 MPa) regimes during compressive creep testing (*5*). In analyzing the response of the composites, they concluded that the material response in the low stress regime is controlled by grain boundary sliding inhibited by dispersoids on the grain boundaries. In the high stress regime, creep is controlled by dislocation movement, with the dispersoids acting to inhibit such

motion (e.g., dispersion strengthening). In reaching this conclusion, they note that the testing temperature was sufficiently high such that lattice diffusion was able to relax the matrix restraint imposed by the presence of the nanoparticles and, therefore, composite strengthening did not occur during creep testing.

Similar to room temperature testing, the initial results from elevated temperature testing of Mg nanocomposites indicate that appreciable improvements in mechanical properties can be obtained with minimal additions of nanosized reinforcements. Moreover, the temperature stability is such that the property improvements remain superior to room temperature properties of comparable nanocomposites for moderate increases in temperature. Although much work remains to be done to fully characterize these materials at elevated temperature and in varying environments, these materials possess significant potential for use in applications up to a temperature range of 150–175 °C.

3.6 Oxidation Resistance

In a recent effort, researchers have quantified the influence of 0.66, 1.11, and 1.50 v% alumina nanoparticles on the oxidation resistance of AZ31B (*54*). After processing by the DMD/extrusion process, the weight gain due to oxidation of the nanoreinforced samples was measured using a DTA-TG equipped with a scale accurate to 1 μg. Samples were heated at a rate of 50 °C/min to a test temperature in the range of 300–470 °C for a hold time up to 7 h. Experimental results indicate that the alumina nanoparticles were effective in retarding the rate of oxidation over the entire temperature range used, with the effectiveness increasing in direct correlation with nanoparticle content. However, the presence of the nanoparticles could not prevent a transition from parabolic to linear oxidation kinetics at 450 °C. Such a transition is indicative of a porous and/or cracked oxide layer that is no longer capable of protecting the alloy from further oxidation.

3.7 Summary

In summary, it is clear that the addition of nanosized reinforcements—whether ceramic, metallic, or a combination of the two—can have a dramatic effect on the performance of Mg. Certainly, this improvement is most obvious in significantly improved tensile properties, which result from the reduction in grain size of the Mg matrix, as well as the strengthening effects of the nanoparticles. However, improvement is also observed in properties such as microhardness, in addition to wear and oxidation resistance. Finally, the presence of ceramic nanoparticles also resulted in the retention of improved properties at elevated temperatures due to the higher thermal stability of the ceramic nanoparticles. Not surprisingly, experimental results indicated that the property enhancements are influenced by the degree and uniformity of nanoparticle dispersion which is, in turn, influenced by the processing method used in producing the nanocomposite. Consequently, the manufacture of nanoreinforced Mg sheet and/or components will require a concentrated effort to develop primary and secondary processing methods that achieve the uniform dispersion of the nanoreinforcements.

4. Army-related Applications

The consideration of Mg for use in a variety of Army-related applications is not a recent occurrence, as detailed by Mathaudhu and Nyberg in their review of the historical, current, and potential use of Mg in military applications (*55*). In particular, they detailed how the use of Mg changed from a widely used structural material, as demonstrated by the more than 12,000 lbs. used in various ways in the B-36 Peacemaker and B-47 Stratojet, to a material primarily used in specialty applications, such as transmission and gear housings in the Sikorsky Black Hawk helicopter. The majority of this downward pattern had occurred by the 1950s and 60s, when more demanding performance requirements revealed the shortcomings then associated with Mg alloys. Several factors were given for this downward trend: poor mechanical properties, perceived flammability issues, and environmental corrosion problems.

However, as indicated previously, continual research and development of Mg alloys has successfully addressed each of these concerns, thereby producing a range of alloys with the desired levels of corrosion resistance and mechanical properties. Indeed, Cho et al. have reviewed the current state of Mg development for Army-related ground vehicle applications (*56*). Two Mg alloys—WE43 and Elektron 675—currently under development through a cooperative agreement between the U.S. Army Research Laboratory (ARL) and Magnesium Elektron, NA show great promise for a variety of applications. WE43 has superior corrosion resistance to many early Mg alloys and is being considered for a variety of applications. Elektron 675 is designed to have superior mechanical properties at elevated temperatures. Initial results indicate that it has twice the strength of aluminum at 200 °C, while weighing half as much as titanium. Work is progressing on both alloys to achieve the desired level of processing knowledge, mechanical characterization, and design experience required to incorporate Mg into widespread usage.

Despite these noticeable advances, barriers still remain in the widespread use of Mg in military applications. In the recent International Magnesium Workshop, a panel of scientists and engineers examined the potential of Mg alloys for applications in numerous ground and air vehicles (*57*). Of particular importance, this report highlighted the need to raise yield strengths to 350 MPa in the near term, with a long-term goal of 500 MPa, while maintaining a ductility equal to or greater than 10%. Other areas of concern that were identified include the need to develop models for microstructural evolution and alloy design; to acquire mechanical property data for high strain rate and/or ballistic testing; to improve the poor corrosion, fatigue, and creep performance of Mg; and to allay the misperception that ballistic impact of Mg will result in explosive conditions.

Based on the results presented herein, it is clear that nanoreinforced Mg offers a viable approach for reaching many of the property improvements outlined by the International Magnesium

Workshop. Indeed, the yield strength of high-strength alloy ZK60A is approximately 300 MPa in the T5 condition. Supposing that the addition of nanoparticles increases the yield strength of the alloy by as little as 20%, the desired yield strength of 350 MPa is easily reached and the higher value of 500 MPa is distinctly possible. Although additional research is needed to understand the influence of nanoparticles on Mg alloys rather than elemental Mg, initial results obtained from nanocomposites based on AZ31B, AZ61, and AZ91 indicate that an improvement in tensile properties also occurs in Mg alloys (*33, 35, 49, 58*). In these studies, sizeable improvements were observed in yield strength (14% to 100%) and ultimate strength (7% to more than 50%), while the strain to failure was equivalent or, in some cases, up to 113% higher than the non-reinforced alloys.

With regard to Army applications, the ability to produce the nanoreinforced material in sufficient quantity is clearly a determinant of its potential use. Many reports surveyed for this review used scaled-down samples (for example, 25 mm long × 5 mm diameter tensile specimens) obtained from lab scale processing efforts. Obviously, there is a need to transition from lab quantities to the production of large rolls and/or sheets of material. Each of the "family" of processing methods has significant disadvantages to be overcome in order to make this transition. In the case of the powder-based approaches, it is fairly easy to envision the production of large scale rolls through the simple mixing of powders prior to rolling and/or forging. However, experimental results consistently indicate that tensile properties obtained from this method are lower than those measured in samples produced from melt-based methods due to the poorer dispersion of the nanoparticles in the powder-based materials. In considering the melt-based processing methods, the DMD method produces nanocomposites with significantly improved properties. However, this advantage is offset by the increased costs and time associated with the production and collection of the metal droplets. Although stir casting is a more direct processing route, this method also has difficulties, primarily in achieving the uniform dispersion of nanoparticles throughout the Mg matrix by preventing segregation to the grain boundaries during casting. Of the various methods, casting, when viewed in terms of commercial viability, has a marginal advantage due to its compatibility with existing manufacturing infrastructure and the ability to produce larger lot sizes (*47*).

Assuming that an appropriate processing method can be established, what are the potential areas where nanoreinforced Mg can make a significant impact on the material needs of the U.S. Army? An instance in which Mg is under serious consideration is in engine blocks and housings for the Fuel Efficient Ground Vehicle Demonstrator currently under development by the U.S. Army Tank and Automotive Research, Development, and Engineering Center (TARDEC) (*55*). A central theme of this program is to lower fuel requirements by developing a tactical vehicle with superior fuel economy relative to the M114 HMMWV. Similarly, the use of Mg for various components, such as gear housings, in tactical wheeled vehicles is also under consideration.

As indicated earlier, Mg alloys have been used in the transmission and gear housing of Sikorsky Black Hawk helicopters. The continued improvement in both physical and mechanical properties

for Mg alloys has enabled its use in the next generation of helicopters, as demonstrated by the use of WE 43 alloy in transmission casings in new commercial helicopter programs, such as the Eurocopter and Sikorsky S92 (*59*). It would not be surprising for this alloy, or perhaps a nanoreinforced Mg alloy, to transition to similar applications on military helicopters.

One area that has seen a reverse trend in the use of Mg is ballistic protection. Ballistic testing of ―Dowmetal" (Mg-Al-Mn alloy now labeled as ―AM" series) in the early 1940s indicated that it had a perforation resistance poorer than either face-hardened steels or age-hardenable aluminum alloys (*55*). Following the development of a new generation of Mg alloys, there is a renewed interest in Mg alloys for lightweight armor applications. Indeed, an approximate three-year program of extensive development and ballistic testing of alloy AZ31B resulted in the recent publication of MIL-DTL-32333, the first Mg armor plate military specification (*60, 61*). Results obtained during ballistic testing indicated that AZ31B was comparable to that of aluminum alloy 5083 with the exception of the 20 mm fragment simulating projectiles. In this case, the aluminum alloy performed approximately 20% better than the Mg alloy. These results were both encouraging and surprising, as AZ31B is designed for general usage and not ballistic applications. Subsequent testing of WE43 plate indicated that it had superior ballistic performance than AZ31B (*56*). Efforts are underway to determine the ballistic performance of additional high-strength wrought Mg alloys.

Similarly, there is also a growing interest in the use of Mg alloys in the area of personnel protection, as evidenced by work examining the potential use of Mg in helmet designs (*62*) as well as body armor. Factors driving this growing interest are high values for specific strength and stiffness, as well as excellent damping characteristics. A further factor in the consideration of Mg in this developmental work is the ability to use superplastic forming to shape Mg sheets into the form required for helmet or body armor designs.

Finally, a general area where the introduction of Mg nanocomposites could have a significant impact on performance is in the replacement of aluminum alloys. While it is true that any replacement effort would have to be evaluated on a case by case basis, it is conceivable that a Mg nanocomposite could offer similar mechanical properties, while offering an approximate 33% reduction in weight. Thus, it is clear that the use of Mg nanocomposites offers scientists and engineers a valid option in the ongoing drive at lightweighting Army vehicles and systems.

5. Conclusions

Although Mg has always held much promise, concerns regarding its corrosion resistance, flammability, and poor workability, among others, have prevented it from widespread incorporation into actual components. Extensive research and alloy development have solved the majority of these issues. As a result, engineers are reevaluating the potential of Mg alloys in a

broad range of applications, especially where the light weight and high specific properties of Mg offer tangible benefits over existing materials.

This renewed interest, combined with the ready availability of both metallic and ceramic nanoparticles, has resulted in widespread research into the production and properties of Mg-based nanocomposites. Experimental results indicate that significant improvements in properties can be obtained with the minimal additions of nanoparticles. Indeed, many reports show that the best combination of strength and ductility are achieved following the addition of approximately 0.6 v% nanoparticles. Strength improvements on the order of 30–50% were common, while ductility improvements over 100% have also been reported. Theoretical analysis has found that the improvement in tensile properties results from the interaction of the nanoparticles with moving dislocations (Orowan strengthening), and the thermally induced stresses caused by differences in thermal expansion coefficient. Sizeable improvements in many other properties, such as microhardness, compression, creep, and wear resistance, were also observed.

Interest in Mg within the U.S. Army has grown as a direct result of the development of the new generation of Mg alloys. On their own, these alloys have the potential for use in a broad array of applications where lightweight materials are required. The incorporation of nanoparticles to form Mg-based nanocomposites, with the resulting property improvements, expands the potential use of these materials to areas not previously considered for Mg-based alloys. Although the materials show much promise, work remains to be done in the areas of fatigue and tensile creep performance. Furthermore, from an Army perspective, efforts are also needed to identify processing routes that are capable of producing material in the quantities sufficient for Army-related activities. Provided these issues are satisfactorily resolved, there is every reason to believe that nanoreinforced Mg can play an important role in meeting the current and future materials need of the U.S. Army.

6. References

1. Kainer, K. U.; Von Buch, F. In: Kainer KU (ed) Magnesium-Alloys and Technologies, Wiley-VCH, Weinheim, 2, 2003.
2. Ye, H. Z.; Liu, X. Y. *J Mater Sci* **2004**, *29*, 6153–6171.
3. Hwang, S.; Nishimura, C.; McCormick, P. G. *Scripta Mater* **2001**, *44*, 2457–2462.
4. Hassan, S. F.; Gupta, M. *Mater Sci Eng* **2005**, *A392*, 163–168.
5. Hassan, S.F.; Gupta, M. *J Mater Sci* **2006**, *41*, 2229–2236.
6. Thein, M. A.; Lu, L.; Lai, M. O. *Compos Struct* **2006**, *75*, 206–212.
7. Hassan, S. F.; Gupta, M. *Mater Sci Eng* **2006**, *A425*, 22–27.
8. Garcés, G.; Rodriguez, M.; Perez, P.; Adeva, P. *Compos Sci Technol* **2007**, *67*, 632–637.
9. Zhong, X. L.; Wong, W.L.E; Gupta, M. *Acta Mater* **2007**, *55*, 6338–6344.
10. Hassan, S. F.; Gupta, M. *J Eng Mater Technol* **2007**, *129*, 462–467.
11. Tun, K. S.; Gupta, M. *Compos Sci Technol* **2007**, *67*, 2657–2664.
12. Tun, K. S.; Gupta, M. *J Mater Sci* **2008**, *43*, 4503–4511.
13. Thein, M. A.; Lu, L.; Lai, M. O. *J Mater Process Technol* **2009**, *209*, 4439–4443.
14. Prasad, Y.V.R.K.; Rao, K. P.; Gupta, M. *Compos Sci Technol* **2009**, *69*, 1070–1076.
15. Hassan, S. F.; Gupta, M. *Compos Struct* **2006**, *72*, 19–26.
16. Ferkel, H.; Mordike, B. L. *Mater Sci Eng* **2001**, *A298*, 193–199.
17. Gupta, M.; Wong, W.L.E. *Scripta Mater* **2005**, *52*, 479–483.
18. Tun, K. S.; Gupta, M. *J Alloy Compd* **2008**, *466*, 140–145.
19. Tun, K. S.; Gupta, M. *J Alloy Compd* **2009**, *287*, 76–82.
20. Wong, W.L.E.; Gupta, M. *Compos Sci Technol* **2007**, *67*, 1541–1552.
21. Cao, G.; Konishi, H.; Li, X. *Mater Sci Eng* **2008**, *A486*, 357–362.
22. Sudarshan, Surappa, M. K.; Ahn, D.; Raj, R. *Metall Mater Trans* **2008**, *39A*, 3291–3297.
23. Cao, G.; Kobliska, J.; Konishi, H.; Li, X. *Metall Mater Trans* **2008**, *39A*, 880–886.

24. Shiying, L.; Feipeng, G.; Qiongyuan, Z.; Wenzhen, L. *Mater Sci Forum* **2009**, *618–619*, 449–452.

25. DeCicco, M.; Konishi, H.; Cao, G.; Choi, H. S.; Turng, L. S.; Perepezko, J. H.; Kou, S.; Lakes, R.; Li, X. *Metall Mater Trans* **2009**, *40A*, 3038–3045.

26. Hassan, S. F.; Gupta, M. *J Alloy Compd* **2006**, *419*, 84–90.

27. Hassan, S. F.; Gupta, M. *J Alloy Compd* **2007**, *429*, 176–183.

28. Hassan, S. F.; Gupta, M. *J Alloy Compd* **2008**, *457*, 244–250.

29. Nguyen, Q. B.; Gupta, M. *J Alloy Compd* **2008**, *459*, 244–250.

30. Nguyen, Q. B.; Gupta, M. *Compos Sci Technol* **2008**, *68*, 2185–2192.

31. Lim, C.Y.H.; Leo, D. K.; Ang, J.J.S.; Gupta, M. *Wear* **2005**, *259*, 620–625.

32. Hassan, S. F.; Tan, M. J.; Gupta, M. *Mater Sci Eng* **2008**, *A486*, 56–62.

33. Paramsothy, M.; Hassan, S. F.; Srikanth, N.; Gupta, M. *Mater Sci Eng 2009*, *A527*, 162–168.

34. Chen, C. Y.; Tsao, Y. A. *Mater Sci Eng* **2004**, *A383*, 21–29.

35. Hung, Y. P.; Huang J. C.; Wu, K. J.; Tsao, C.Y.A. *Mater Trans* **2006**, *47*, 1985–1993.

36. Goh, C. S.; Wei , J.; Lee, L. C.; Gupta, M. *Acta Mater* **2007**, *55*, 5115–5121.

37. Lan, J.; Yang, Y.; Li, X. *Mater Sci Eng* **2004**, *A386*, 284–290.

38. Habibnejad-Korayem, M.; Mahmudi, R.; Gasemi, H. M.; Poole, W. J. *Wear* **2010**, *268*, 405–412.

39. Habibnejad-Korayem, M.; Mahmudi, R.; Poole, W. J. *Mater Sci Eng* **2009**, *A519*, 198–203.

40. Zhang, Z.; Chen, D. L. *Scripta Mater* **2006**, *54*, 1321–1326.

41. Zhang, Z.; Chen, D. L. *Mater Sci Eng* **2008**, *A483–484*, 148–152.

42. Wang, X. L.; Yu, Y.; Wang, E. D. *Mater Sci Forum* **2005**, *488–489*, 535–538.

43. Mukai, T.; Yamanoi, M.; Watanabe, H.; Higashi, K. *Scripta Mater* **2001**, *45*, 89–94.

44. Hassan, S. F.; Tan, M. J.; Gupta, M. *Mater Sci Tech* **2007**, *23*, 1309–1312.

45. Lim, S.C.V.; Gupta, M. *Mater Res Bull* **2001**, *26*, 2627–2636.

46. Ugandhar, S.; Gupta, M.; Sinha, S. K. *Compos Struct* **2006**, *72,* 266–272.

47. Friedrich, H. E.; Mordike, B. L. *Magnesium Technology – Metallurgy, Design Data, Applications*, Springer, Berlin, 606, 2006.

48. Thakur, S. K.; Srivatsan, T. S.; Gupta, M. *Mater Sci Eng* **2007**, *A466*, 32–37.

49. Nguyen, Q. B.; Gupta, M. *Mater Sci Eng.* 2010, DOI:10.1016/j.msea.2009.11.002.

50. Garcés, G.; Rodriguez, M.; Adeva, P. *Mater Sci Eng* **2006**, *A419*, 357–364.

51. Nguyen, Q. B.; Gupta, M. *J Alloy Compd*. **2010**, DOI:10.1016/j.jallcom.2009.09.188.

52. Hwang, S.; Nishimura, C.; McCormick, P. G. *Scripta Mater* **2001**, *44*, 2457–2462.

53. Han, B. Q.; Dunand, D. C. *Mater Sci Eng* **2001**, *A300*, 235–244.

54. Nguyen, Q. B.; Gupta, M.; Srivatsan, T. S. *Mater Sci Eng* **2008**, *A500*, 233–237.

55. Mathaudhu, S.; Nyberg, E. unpublished manuscript, 2010.

56. Cho, K.; Sano, T.; Doherty, K.; Yen, C.; Gazonas, G.; Montgomery, J.; Moy, P.; Davis, B.; DeLorme, R. Magnesium Technology and Manufacturing for Ultra Lightweight Armored Ground Vehicles. *Proceedings of the 2008 Army Science Conference* 2008.

57. Ma, E.; Ramesh, K. T.; Dowding, R.; McCauley, J. W. *International Magnesium Workshop*; ARL-SR-162; U.S. Army Research Laboratory: Aberdeen Proving Ground, MD, 2008.

58. Ho, K. F.; Gupta, M.; Srivatsan, T. S. *Mater Sci Eng* **2004**, *A369*, 302–308.

59. Magnesium in Aerospace Magnesium Elektron, Swinton, Manchester, UK, 2009. http://www.magnesium-elektron.com/markets-applications.asp?ID=8. accessed 11 January 2010.

60. Jones, T. L.; DeLorme, R. D.; Burkins, M. S.; Gooch, W. A. *Ballistic Evaluation of Magnesium Alloy AZ31B*; ARL-TR-4077; U.S. Army Research Laboratory: Aberdeen Proving Ground, MD, 2007.

61. Jones, T. L.; DeLorme, R. D. *Development of a Ballistic Specification for Magnesium Alloy AZ31B*; ARL-TR-4664; U.S. Army Research Laboratory: Aberdeen Proving Ground, MD 2008.

62. Walsh, S. M.; Scott, B. R.; Jones, T. L.; Cho, K.; Wolbert, J. A Materials Approach in the Development of Multi-Threat Warfighter Head Protection. *Proceedings of the 2008 Army Science Conference*, 2008.

List of Symbols, Abbreviations, and Acronyms

Material Specific

Al_2O_3	Aluminum Oxide or Alumina
Ar	argon
CNT	Carbon Nanotubes
Cu	copper
CP Mg	Commercially Pure Magnesium
Fe	iron
Mg	magnesium
Nd	neodymium
SiC	Silicon Carbide
SiO_2	Silicon Dioxide or Silica
TiC	Titanium Carbide
Y	yttrium
Y_2O_3	Yttrium Oxide or Yttria
ZrO_2	Zirconium Oxide or Zirconia

General

ARL	Army Research Laboratory
BPS	Blend-Press-Sinter
CTE	Coefficient of Thermal Expansion
DMD	disintegrated Melt Deposition
DTA-TG	Differential Thermal Analysis and Thermal Gravimetry Analysis
FESEM	Field Emission Scanning Electron Microscope
HCP	Hexagonal Close Packed

MPa	Megapascal
TARDEC	Tank and Automotive Research, Development, and Engineering Center
v%	Volume Percent
w%	Weight Percent

ADMNSTR
DEFNS TECHL INFO CTR
ATTN DTIC OCP (ELECTRONIC COPY)
8725 JOHN J KINGMAN RD STE 0944
FT BELVOIR VA 22060-6218

US ARMY RSRCH LAB
ATTN RDRL WMM F V H HAMMOND
BLDG 4600
ABERDEEN PROVING GROUND MD 21005

US ARMY RSRCH LAB
ATTN IMNE ALC HRR MAIL & RECORDS MGMT
ATTN RDRL CIO LL TECHL LIB
ATTN RDRL CIO MT TECHL PUB
ADELPHI MD 20783-1197